Leveraging Kernelized Synergies on Shared Subspace for Precision Grasping and Dexterous Manipulation

Sunny Katyara 🅙 , *Student Member, IEEE*, Fanny Ficuciello 🅙 , *Senior Member, IEEE*, Darwin G. Caldwell 🅙 , *Senior Member, IEEE*, Bruno Siciliano 🅙 , *Fellow, IEEE*, and Fei Chen 🅙 , *Senior Member, IEEE*

Abstract—Manipulation in contrast to grasping is a trajectorial task that needs to use dexterous hands. Improving the dexterity of robot hands, increases the controller complexity and thus requires to use the concept of postural synergies. Inspired from postural synergies, this research proposes a new framework called kernelized synergies that focuses on the re-usability of same subspace for precision grasping and dexterous manipulation. In this work, the computed subspace of postural synergies is parameterized by kernelized movement primitives to preserve its grasping and manipulation characteristics and allows its reuse for new objects. The grasp stability of proposed framework is assessed with the force closure quality index, as a cost function. For performance evaluation, the proposed framework is initially tested on two different simulated robot hand models using the Syngrasp toolbox and experimentally, four complex grasping and manipulation tasks are performed and reported. Results confirm the hand agnostic approach of proposed framework and its generalization to distinct objects irrespective of their dimensions.

Index Terms—Postural synergies, Kernel trick, Anthropomorphic hands, Dexterous manipulation, Probabilistic learning

I. INTRODUCTION

FOR more than three decades, roboticists have been actively trying to replicate the dexterity of the human hand and there have been excellent developments in the field of dexterous robot hands and advanced controls [1][2]. But these robot hands have failed to achieve the universality and subtle behavior that characterizes the dexterous manipulation, due to the limitations of available software and hardware. Building robot hands for dexterous manipulation that can emulate or even approach the functionality of humans is challenging owing to the fact that available sensors and actuators are not equivalent in size, precision and accuracy to the human muscles and skin. Dexterous manipulation epitomizes the ability

Sunny Katyara is with ADVR, Istituto Italiano di Tecnologia, Italy PRISMA Lab, University of Naples Federico II, Italy and Electrical Engineering, Sukkur IBA University, Pakistan (e-mail: sunny.katyara@iit.it).

Fanny Ficuciello and Bruno Siciliano are with Department of Information Technology and Electrical Engineering and PRISMA Lab, University of Naples Federico II, Naples, Italy (e-mail: name.surname@unina.it).

Darwin Caldwell is with Department of Advanced Robotics, Istituto Italiano di Tecnologia, Genova, Italy (e-mail: darwin.caldwell@iit.it).

Fei Chen is with Department of Mechanical and Automation Engineering, T-Stone Robotics Institute, The Chinese University of Hong Kong, Hong Kong (e-mail: f.chen@ieee.org).

Fig. 1: Representation of precision grasp and dexterous manipulation

of hands to change the object pose from one configuration to another and can be achieved by re-grasping, finger gaiting and rolling/sliding [3].

Dexterous manipulation by finger gaiting inherently depends upon the stability and configuration of the precision grasp to determine the minimum number and optimal position of the fingertips on the object's surface, as shown in Fig. 1. However, this is an iterative process and to avoid having to compute the optimal grasp each time, a database of grasps can be created and exploited to sample and rank the candidate grasps [4][5][6]. But, the grasp configurations do not only depend upon the object but the robot as well. When the robot has a greater number of degrees of freedom (DOF), the controller complexity increases. To simplify the control of dexterous hands, inspiration is taken from the neuro-scientific behavior of the human brain, that suggests the use of postural synergies [7][8]. Postural synergies form a reference subspace of coordinated human movements that are related to the hand kinematics. The postural synergies are computed from the joint configurations of the hand using statistical analysis methods such as:-, principal component analysis (PCA), expectation-maximization (EM), factor analysis and other analytical dimensionality reduction techniques [9][10]. In simple words, the postural synergies are the reduced control parameters, used to reproduce certain hand postures without regulating each joint individually. They are represented by a couple (E, e).

Postural synergies computed on human hands require a mapping strategy to overlay the corresponding synergistic motions onto the kinematics of robot hands. There are three major mapping algorithms i.e, joint-joint mapping, Cartesian-space mapping and object-based mapping [11][12]. However, all of these are prone to errors due to dissimilarity in the kinematics and dimensions of the human and robot hands. Therefore, robot hands are either tele-operated during tasks or kinesthetically taught the required skills by a human expert

[13][14] and the statistical analysis is directly applied to the robot hand configurations to extract the synergy subspace. Such a direct use of postural synergies is one of the most common manipulation strategies used in robot learning [15].

Although, postural synergies have been effectively exploited in grasping of distinct objects with different robot hand designs [16][17]. Their application to dexterous manipulation, which requires continuous coordination among all the fingers, brings many challenges especially (i) ensuring the close form stability of the grasping posture, (ii) exploiting smaller but preferably the same number of control parameters for both the actions i.e, grasping and manipulation and (iii) computing and utilizing the synergistic subspace irrespective of the dimensions of the objects or the configurations of the robot hands. Nonetheless, a few attempts have been made to use postural synergies for manipulation as well [18][19] but generally they have not been effective as they require additional synergies to be used for different scenarios. This, of course violates the prime motivation behind their use i.e, simplifying the robot hand control. Such limitations of postural synergies for continuous trajectorial tasks, confirm a marginal gap between the grasping and manipulation sub-spaces and thus require the introduction of middle-ware to link them. The development of a uniform synergistic subspace with the application of middle-ware, defines the problem addressed in this research. However, the possible intermediate link could be achieved through the use of a probabilistic kernel trick, which is an instance based learning approach rather than having to learn some fixed set of parameters [20]. The probabilistic kernel approach strongly preserves the grasping and manipulation primitives of the computed synergy subspace globally and allows its reuse for different interaction tasks on unknown objects if their poses could be correctly estimated. This is the main motivation behind the development of our framework, which has been termed "Kernelized Synergies". The conceptual representation of kernelized synergies on a shared grasping and manipulation subspace is shown in Fig. 2. It shows how the same subspace may be shared between the grasping and manipulation components to execute the desired actions on the object.

The rest of this paper is organized as follows; Section-III discusses the recent research work in the field of postural synergies and the major contributions of this research. Section-IV presents the research methodology on the formulation of kernelized synergies. Section-V details the grasp stability analysis using the force closure property together with the soft synergy model for contact compliance. Section-VI evaluates the performance of kernelized synergies when applied to two different simulated robot hand models in the SynGrasp toolbox. Section-VII examines the experimental results obtained using kernelized synergies in four different complex scenarios and section-VIII gives the final conclusions about the development, application and outcome of the proposed framework and its possible extensions to the future work.

II. RELATED WORKS AND OUR CONTRIBUTIONS

For stable grasping and dexterous manipulation, a robot hand must exploit the dimensions of the object and environmental constraints and a method to address this was introduced
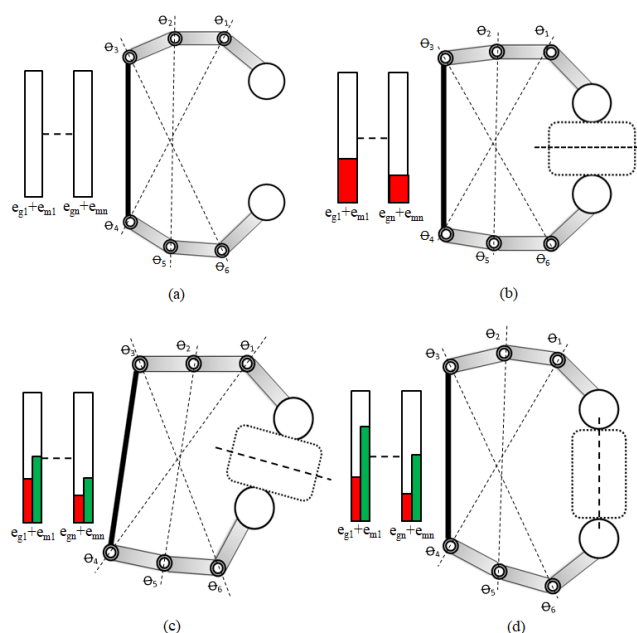

Fig. 2: Conceptual representation of kernelized synergies on the shared subspace for grasping (g) and manipulation (m), (a) represents the zero-offset pose of a hand with corresponding synergies in columns, (b) is the grasping pose obtained at respective values of synergies (red), (c) denotes the manipulation (continual rotation) of a grasped object by co-utilizing the grasping subspace (red) and manipulation parameters (green), (d) shows the quadrature rotation of grasped objects achieved with the combination of corresponding manipulation synergies (green). The dotted lines indicate the coordination among the hand joints in the synergistic subspace.

in [21]. It used tactile information with postural synergies to make a trade-off between the controller complexity and kinematic redundancy. This work was limited to the grasping of known objects in an unstructured environment. However, to automate and improve the synergy based grasping, a framework was discussed in [22]. It was restricted to synergistic grasping and did not examine manipulation. Hence, to exploit the synergy subspace also for manipulation, a technique was presented in [23] that employed additional synergies for manipulation but this increased the controller complexity while failing to adapt to different dimensions of known objects. Therefore, to add adaptive characteristics to postural synergy components and benefit from their smaller number, a new design and control architecture for hands was proposed in [24]. The developed architecture with only two synergies was able to perform grasping and manipulation of a large variety of objects. Yet, the framework was hand dependent as intelligence was embodied into its mechanical structure and it was unable to achieve the required system dynamics. So, to address the uncertainties related to the system dynamics during manipulation, a dynamic approach was presented in [25]. This approach used a kernel technique indirectly to estimate variations in the geometrical properties of manipulated object but it suffers from dimensionality due to the inverse cubic dependence of its kernel matrix. However, the promising potential of this concept motivated us to use a kernel trick on postural synergies and to extend this to dexterous manipulations as well.

To the best of our knowledge, there is no single control

TABLE I: Comparison among the existing state-of-art techniques and proposed framework.

Parameter	Soft synergies [18]	Manipulation synergies [19]	Complex synergies [23]	Our approach
Task general-ization	✓	×	×	✓
Object adaptation	✓	×	×	✓
Subspace retention	×	✓	×	✓
Task prioritization	×	×	×	✓
Properties preservation	✓	×	✓	✓
Grasping & manipulation	×	✓	✓	✓

Task generalization: perform tasks on new objects outside the data set
Object adaptation: adapt to the size and shape of different objects
Subspace retention: same subspace used for grasping & manipulation
Task prioritization: give preferences to tasks based on their priority levels
Properties preservation: preserve the grasping properties of the subspace
Grasping & manipulation: able to grasp and then manipulate objects

framework available to share the same reduced subspace for precision grasping and dexterous manipulation and this is a key to the development of kernelized synergies. The major contributions and main objectives of this research are; (1) to extract postural synergies for robot hand postures corresponding to grasping and manipulation of training objects and apply Gaussian Mixture Model (GMM) together with Gaussian Mixture Regression (GMR) to obtain a unified reference synergistic trajectory, that can be used to reproduce and generalize the learned skills, (2) to exploit Kernelized Movement Primitives (KMP), that inherently kernelizes the computed synergistic subspace so that the learned skills are preserved globally and can be reused for unknown objects, (3) to incorporate a force closure quality index as a cost function to measure the success and stability of grasps established using the kernelized synergies, and (4) to evaluate the performance, robustness, and reproducibility of the proposed framework under complex interaction scenarios. This is at first tested on two different simulated robot hand models in the Syngrasp toolbox and later on a real anthropomorphic robot hand for four distinct tasks i.e, pouring coffee and closing a jar, opening toolbox latches, grasping and manipulating two objects sequentially, and playing the board game "carrom".

To better understand the capabilities of the proposed framework, a comparison is made with other state of art approaches, used for synergistic grasping and manipulation in Table. I.

III. RESEARCH METHODOLOGY

A. Proposed Framework

Figure 3 represents the block diagram of the proposed methodology to perform robust, reliable and adaptive grasping and manipulation with the dexterous robot hand. The methodology starts with teaching basic grasping and manipulation primitives to the robot hand using the training objects in Fig. 4 and recording the corresponding hand joint configurations q. The vectors of mean hand joints ϑ corresponding to the
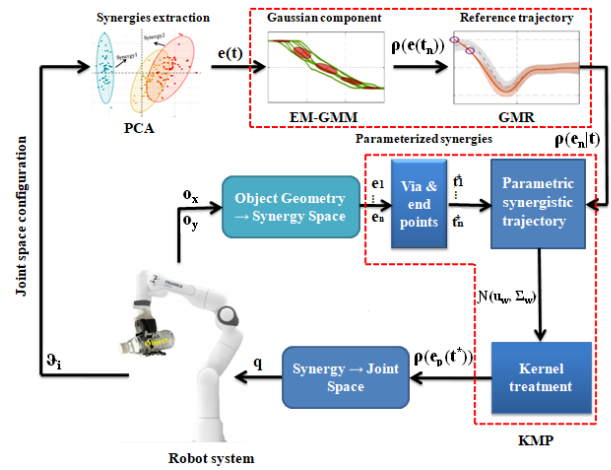

Fig. 3: Block diagram of proposed methodology on the formulation and development of kernelized synergies framework.

recorded hand joint configurations are normalized using PCA and the respective eigen vectors, called postural synergies (E, e), are extracted. The coefficients of computed postural synergy e evolve over the duration of the demonstrations to provide the corresponding synergistic trajectories $e(t)$. In order to account for inconsistencies during demonstrations and obtain a generalized probabilistic trajectory to reproduce the learned skills, the GMM is applied to approximate the distribution of synergistic trajectories $\rho(e(t))$ in terms of the Gaussian components. The EM algorithm initializes the Gaussian parameters i.e. weight, mean and co-variance. The GMR subsequently computes the conditional distribution of data in the GMM with respect to partially observed data during EM iterations and outputs the reference trajectory $\rho(e_n|t)$ for the demonstrated synergistic trajectories. In order to adapt to new conditions i.e, new objects, and encode the synergistic trajectories that exhibit time dependent variance, the KMP is exploited to generate a parametric synergistic trajectory $\rho(e_p(t^*))$. The use of the kernel trick (k, K) in the KMP helps to preserve the probabilistic properties (grasping and manipulation primitives) of parametric synergistic trajectory from multiple demonstrations, and alleviates the need for basis functions (ϕ, Φ) to be used to estimate it. Geometrical information of the object o is first translated into its corresponding synergistic data, which is then used to modulate the via points and end points of the reference trajectory and thus the synergy subspace generates the new task trajectory and with it develops the capability to adapt to unknown conditions i.e. new objects. Finally, the mapping from synergy subspace to joint space helps to perform the desired tasks on the robot hand.

B. Nomenclature

The following list provides the description of different variables and parameters used throughout the paper:

- θ, ϑ ⟶ Robot hand joint angles and their vector
- q ⟶ Robot hand joint configuration corresponding to certain posture
- C ⟶ Configuration matrix of mean robot hand postures
- E ⟶ Synergy matrix

- $e_g, e_m \longrightarrow$ Grasping and manipulation synergy coefficient
- $e(t) \longrightarrow$ Interpolated trajectory of synergy coefficient
- $N, M \longrightarrow$ Number of Gaussian components and distributions
- $\pi, \mu, \Sigma \longrightarrow$ prior, mean and covariance of probablistic distribution
- $\Theta(t) \longrightarrow$ Matrix of coefficients of parametric trajectory
- $\phi, \Phi \longrightarrow$ Basis functions (features) and their matrix
- $\lambda \longrightarrow$ Regularization parameter
- $k, K \longrightarrow$ Kernel function and matrix
- $\Upsilon \longrightarrow$ Priority coefficient
- $A_m \longrightarrow$ Motion transfer matrix
- $p, o \longrightarrow$ Position of robot hand contact points and object
- $n_c.n_q, n_s \longrightarrow$ Number of robot hand contact points, joints, and synergy coefficients
- $J_h \in \mathbb{R}^{n_c \times n_q} \longrightarrow$ Robot hand Jacobian matrix
- $C_h \in \mathbb{R}^{n_q \times n_q} \longrightarrow$ Robot hand joint compliance matrix
- $f_c \in \mathbb{R}^{3n_c} \longrightarrow$ Vector of robot hand contact forces
- $G \in \mathbb{R}^{n_c \times n_c} \longrightarrow$ Robot hand grasp matrix
- $\xi \in \mathbb{R}^3 \longrightarrow$ Vector of robot hand internal forces
- $\omega \in \mathbb{R}^6 \longrightarrow$ Vector of external spatial forces
- $\Gamma(\omega, e) \longrightarrow$ Cost function evaluating grasp stability

C. Extraction of Grasping and Manipulation Synergies

The postural synergies are the data driven control parameters and are obtained from the statistical analysis (i.e, PCA) of the hand joint configurations. In this research, the data is generated by tele-operating the robot hand to perform a range of precision grasping and dexterous manipulation (rotation and translation) actions on a series of geometrical objects, as shown in Fig. 4. The robot hand is taught basic interaction skills such that the computed synergistic subspace can be generalized to perform different tasks on distinct daily life objects. However, for tele-operation, the keyboard interface is used to actuate the robot hand joints for respective grasping and manipulation actions. Since, a human subject is tele-operating the robot hand for the different tasks, the postures assumed by it mimic the human configurations moderately but are not exact due to dissimilarity in the respective kinematics and dimensions. Moreover, for each object, five attempts are made to ensure that the joint configurations corresponding to robot hand postures are precisely recorded and registered onto the desired configuration matrix C. Note that, there were a few instances when an object lost contact with the hand and was dropped. Such trials were flagged and excluded from the data base used to compute the postural synergies.

Let the vector of robot hand joints be denoted by $\vartheta^k = [\theta_1^k, ..., \theta_{12}^k]$ at the kth training task then the nominal posture of the robot hand for K trials is defined by Eq. 1

$$q_0 = \frac{1}{K}\sum_{k=1}^{K}\vartheta^k \qquad (1)$$

The mean position of the robot hand is determined by subtracting the nominal posture from its current joint configuration $\hat{\vartheta}^k = \vartheta^k - q_0$ and then concatenating them into a row vector as $C = [\hat{\vartheta}^1 ...... \hat{\vartheta}^K]^T$. The PCA is applied on C and the reduced subspace of postural synergies (i.e, the subset of

Fig. 4: Training data set obtained by tele-operating the robot hand for grasping and manipulation primitives on given geometrical objects. The free hand motions are the contact-less movements with respect to objects for non-prehensile actions.

predominant principal components numerically characterizing the synergistic subspace) $\hat{E}$ is obtained [26].

To reproduce the required posture on the robot hand for a object to be grasped and manipulated, a proper choice of postural synergy co-efficients $(e) = e_{g1} + e_{m1}, e_{g2} + e_{m2}...e_{gn} + e_{mn}$ needs to be made. Thus, the corresponding synergy co-efficients are determined by Eq. 2

$$e = \hat{E}^{\dagger}(\vartheta - q_0) \qquad (2)$$

Where, the matrix $\hat{E}^{\dagger}$ denotes the pseudo inverse of the reduced synergy matrix, which consists of two predominant synergistic components that have a variance greater than or equal to 85%. This condition defines that the 85% of the learned robot hand postures can be reproduced by exploiting just two synergistic components. However, this selection comes with a trade-off between the controller complexity and better reproduction of hand postures i.e, more synergistic components (control variables) generate finer hand configurations, but it then violates the motivation for using postural synergies (i.e, bringing simplicity) [7]. Hence, the projection of each robot hand configuration onto the synergy subspace can be defined as $\hat{\vartheta} = \hat{E}e$.

The subspace of two predominant postural synergies for a 6 DOF INSPIRE robot hand having 12 joints in Fig. 5 (a) [27], computed using training objects in Fig. 4, is graphical shown in Fig. 5 (b and c). It can be seen from Fig. 5 (b and c) that the meta-carpophalangeal, promixal, and interphalangeal joints of the index finger, middle finger and thumb are used in tripod grasping and manipulation of training objects in Fig. 4. In manipulation tasks, especially for translation actions, the medial angles of all the fingers are strongly activated whereas for rotational motions, the proximal angles are actuated with respect to combined values of synergistic components. However, in all the actions, a difference of 0.256 radians on average exists over the hand joint configurations in the synergistic subspace from grasping to manipulation of training objects
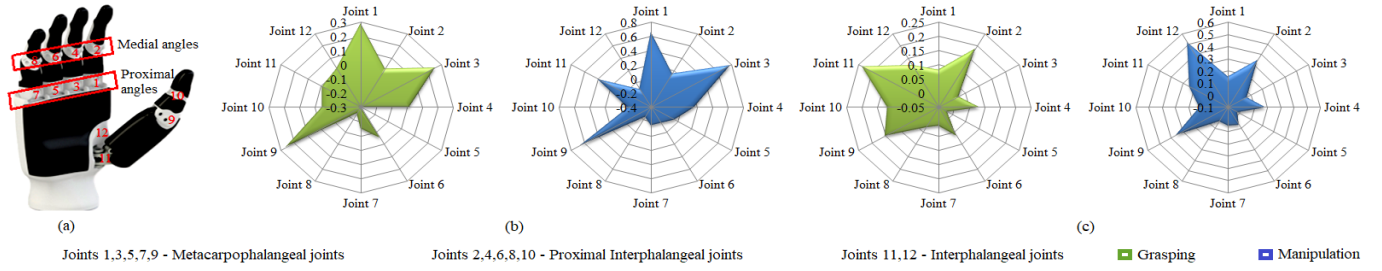
Fig. 5: Polar representation of the computed synergy subspace for a 6 DoF robot hand, (a) is the fully actuated anthropomorphic robot hand, (b) and (c) represent the participation and cooperation of different joints with distinct combined values of first and second synergies using respective grasping and manipulation components.

in Fig. 4. Further, it is evident that the first synergy (with grasping and manipulation components) primarily regulates the promixal and medial angles of all the fingers and the second synergy mainly controls the movements of the thumb and index finger for respective interaction tasks. Moreover, the relative positions of the thumb and index finger help in moving from one grasping posture to another while manipulating an object.

D. Parameterization and Kernelization of Postural Synergies

The synergistic co-efficients e determined in the previous section for each training object in Fig. 4, are evolved over the duration of the demonstrations t to obtain the corresponding synergistic trajectories $e(t)$. In order to capture the joint probabilistic distributions of these synergistic trajectories, a GMM is applied and is defined by Eq. 3 [28][29]

$$\begin{bmatrix} t \\ e \end{bmatrix} \sim \sum_{n=1}^{N} \pi_n \mathcal{N}(\mu_n, \Sigma_n) \qquad (3)$$

Moreover, to generate a reference synergistic trajectory $(\hat{e})_n{}^N = 1$ to be followed by the robot hand to reproduce the taught demonstrations, GMR is applied. This actually defines the conditional joint probability distribution of the GMM i.e, $e_n|t \sim \mathcal{N}(\hat{\mu}_n, \hat{\Sigma}_n)$. The conditional mean $\hat{\mu}_n$ and covariance $\hat{\Sigma}_n$ of the reference synergistic trajectory are thus computed by Eq. 4, where $\mu_n{}^t$ and $\Sigma_n{}^{tt}$ represent the instantaneous mean and co-variance respectively.

$$\hat{\mu}_n = \sum_{n=1}^{N} \frac{\pi_n \mathcal{N}(t_n|\mu_n{}^t \Sigma_n{}^{tt})}{\sum_{n=1}^{N} \mathcal{N}(t_n|\mu_n{}^t \Sigma_n{}^{tt})} \mu_n{}^e + \varrho$$

$$\hat{\Sigma}_n = \sum_{n=1}^{N} \frac{\pi_n \mathcal{N}(t_n|\mu_n{}^t \Sigma_n{}^{tt})}{\sum_{n=1}^{N} \mathcal{N}(t_n|\mu_n{}^t \Sigma_n{}^{tt})} \varphi + \varepsilon \qquad (4)$$

where;
$\varrho = \sum_n{}^{et} (\sum_n{}^{tt})^{-1}(t_n - \mu_n]^t$
$\varphi = (\sum_n{}^{ee} - \sum_n{}^{et}(\sum_n{}^{tt})^{-1}\sum_n{}^{te})$
$\varepsilon = (\mu_n{}^e + \sum_n{}^{et}(\sum_n{}^{tt})^{-1}(t_n - \mu_n{}^t)(\sum_n{}^{tt})^{-1}(t_n - \mu_n{}^t)^T - (\hat{\mu_n})(\hat{\mu_n})^T$

To generalize the learned synergistic subspace to a wider set of objects, the KMP [30] is exploited to generate a parametric synergistic trajectory $e_p(t)$ and is defined by Eq. 5, where μ_w and Σ_w are the weighted mean and co-variance respectively.

$$e_p(t) \sim \mathcal{N}(\Theta(t)^T \mu_w, \Theta(t)^T \Sigma_w \Theta(t)) \qquad (5)$$

The goal of the parametric synergistic trajectory in Eq. 5 is to follow the reference synergistic trajectory in Eq. 4 and to do so, the Kullback-Leibler (KL) divergence criteria is applied, that minimizes the distance between two distributions i.e, $O_{min}(\mu_w, \Sigma_w)$. Hence, the optimal values of weighted mean and co-variance in Eq. 5 are found by Eq. 6 [30], with $\mu = [\hat{\mu}_1, \hat{\mu}_2, ...\hat{\mu}_N]$ and $\Sigma = blockdiag(\hat{\Sigma}_1, \hat{\Sigma}_2, ...\hat{\Sigma}_N)$ representing the mean and co-variance matrices of the demonstrated synergistic trajectories respectively.

$$\mu_w = \Phi(\Phi^T \Phi + \lambda \Sigma)^{-1} \mu$$
$$\Sigma_w = N(\Phi \Sigma^{-1} \Phi^T + \lambda I)^{-1} \qquad (6)$$

To preserve the probabilistic properties of grasping and manipulation synergies so that they can be reused for new objects, and also to alleviate the use of basis functions whose number increases exponentially for complex tasks, Eq. 6 is kernelized in the KMP. The kernel treatment of basis functions used to encode the synergistic trajectory is defined as $k(t_i, t_j) = \phi(t_i), \phi(t_j)$.

Therefore, for any new input t^* (new instance on shape or/and size of object), the expected values of mean and co-variance of the parametric synergistic component are determined by Eq. 7 [30], where $k^* = [k(t^*, t_1), k(t^*, t_2), ...k(t^*, t_N)]$ represents the kernel function for a new object input.

$$\mathbb{E}(e_p(t^*)) = k^*(K + \lambda I)^{-1} \mu$$
$$\mathbb{D}(e_p(t^*)) = \frac{N}{\lambda}(k(t^*, t^*) - k^*(K + \lambda \Sigma)^{-1}k^{*T}) \qquad (7)$$

Moreover, the kernelized synergies framework can also prioritize the different grasping and manipulation tasks on the basis of their assigned weights in the joint probability distribution. For a set of M reference synergistic trajectories, the corresponding synergistic input $\{t_n, \hat{e}_{n,m}\}$ assigned with priority $\Upsilon_{n,m} \in (0,1)$, represented as $\{\{t_n, \hat{e}_{n,m}, \Upsilon_{n,m}\}_{n=1}^{N}\}_{m=1}^{M}$ should satisfy the condition $\sum_{m=1}^{M} \Upsilon_{n,m} = 1$. Therefore, prioritizing the tasks in the kernelized synergy subspace actually corresponds to the product of its M distributions, with $m = 1, 2, ...M$ and is thus explained by Eq. 8 [30]

$$\mathcal{N}(\mu_n{}^T, \Sigma_n{}^T) \propto \prod_{m=1}^{M} \mathcal{N}(\hat{\mu}_{n,m}, \hat{\Sigma}_{n,m}/\Upsilon_{n,m}) \qquad (8)$$

Algorithm 1: Kernelized synergies

input : $\vartheta_i \longrightarrow$ vector of robot hand joints
output: $\rho(e(t)) \backsim$ function$(\mathbb{E}(e(t)), \mathbb{D}(e(t)))$

1 **while** $(\vartheta_i \in \vartheta^k) \longrightarrow C$ **do**
2     $function(C) \longrightarrow (E, e)$;
3   **if** $var(E) \geq 0.85$ **then**
4        $\hat{E}$;
5   **else**
6        $\emptyset \longrightarrow$ null matrix;
7   **end**
8 **end**
9 **forall** $e = \hat{E}^\dagger \hat{\vartheta}$ **do**
10     $\rho(e(t_n)) \backsim \mathcal{N}(\mu_n, \Sigma_n)$
11     $\rho(e_n | t) \backsim \mathcal{N}(\hat{\mu_n}, \hat{\Sigma_n})$
12     $\rho(e_p(t^*)) \backsim function(\mathbb{E}(e(t)), \mathbb{D}(e(t)))$
13   **if** $\Upsilon \neq 0 \longrightarrow priority\ exist$ **then**
14        $\rho(e_p(t)) \backsim \prod^{M} \mathcal{N}(\mu_w, \Sigma_w / \Upsilon)$;
15   **else**
16        $\rho(e_p(t)) \backsim O_{min}(\mu_w, \Sigma_w)$;
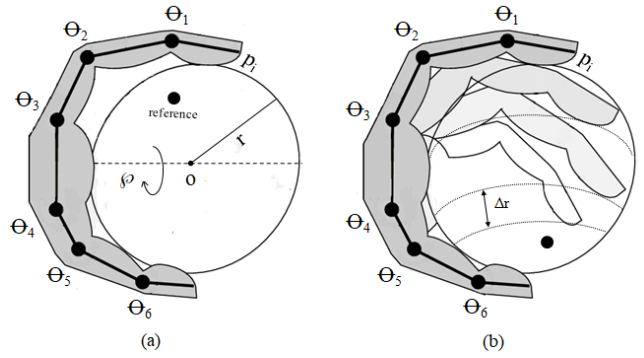17   **end**
18 **end**

Fig. 6: Transformation from task space into synergistic subspace, (a) denotes the translational and angular movement indentations for object grasped by a robot hand, (b) illustrates the possible translation and orientation of the object as it is being manipulated by the hand.

values. A hard finger contact model [31] is considered for the robot-object interaction. Referring to Fig. 6, the relationship between the motion of an object and the contact points of the robot hand manipulating it, is given by Eq. 9 [32]

$$\dot{p} = A_m \begin{bmatrix} \dot{o} \\ \wp \\ \dot{r} \end{bmatrix} \tag{9}$$

Where $\dot{o}$ and $\wp$ represent the linear and angular velocities of the object and $\dot{r}$ denotes the displacement of that object with respect to the position of the contact points p. The motion transfer matrix A_m is defined by Eq. 10

$$A_m = \begin{bmatrix} I & -[p_1 - o]_x & (p_1 - o) \\ \cdots & \cdots & \cdots \\ I & -[p_i - o]_x & (p_i - o) \\ \cdots & \cdots & \cdots \end{bmatrix} \tag{10}$$

In order to determine the corresponding synergistic values, the joint configuration of the robot hand is required. The relation between the robot hand contact points and its joint configuration is defined by the standard differential kinematics $\dot{p} = J_h \dot{\vartheta}$. Therefore, the mapping from hand joint velocities to the corresponding synergistic values is given by Eq. 11

$$\dot{e} = J_h A_m{}^\dagger C_h \hat{E}^\dagger \dot{\vartheta} \tag{11}$$

Where, $A_m{}^\dagger$ is the pseudo inverse of the motion transfer matrix. The compliance matrix C_h defines the free movements of the joints actuated by the respective servos, thereby compensating the friction, damping and shear effects. This matrix is one of the robot hand design parameters and depends upon the mechanical configuration of the joints, the transmission system employed and the type of servos used. For our robot hand, the C_h is determined from its corresponding joint stiffness matrix $K_h = 1.65 I_{12} \frac{Nm}{rad}$ (i.e, $C_h = 1/K_h$), with I_{12} representing a 12×12 identity matrix. The value of K_h is provided by the robot hand manufacturer in the data-sheet [27].

The complete methodology of the kernelized synergies framework is summarized in Algorithm 1. Wherein, the input is the given vector of robot hand joints ϑ_i corresponding to the existing hand joint configuration q. The output is the interpolated values of synergistic coefficients $\rho(e(t))$ in-terms of expected mean $\mathbb{E}(e(t))$ and co-variance $\mathbb{D}(e(t))$. The Algorithm 1 starts by defining the configuration matrix (C) from the mean hand joint configurations $\hat{\vartheta}$ (*line* 2). The function (PCA) is applied to the resultant C to compute the postural synergies (E, e), with the condition that only the synergistic components having variance greater than or equal to 85% should be considered and thus the reduced synergy matrix $\hat{E}$ is obtained (*line* 3, 4, 5, 6, 7), with reference to Eq. 2. For all the synergistic components, the synergistic trajectories $\rho(e(t_n))$ are determined (*line* 10), according to Eq. 3 and approximated using GMM-GMR to generate a single reference trajectory $\rho(e_n | t)$ (*line* 11), based on Eq. 4. With the given reference trajectory, the parametric trajectory for a new object is defined and kernelized using KMP in-terms of expected mean and co-variance $\rho(e_p(t^*))$ (*line* 12), related to Eq. 7. However, if the priorities Υ exist in the given task, the resultant synergistic trajectory is the product of M reference trajectory distributions (*line* 14), referring to Eq. 8. Otherwise, it is based on minimizing the distance between the parametric and reference trajectories to perform the desired task (*line* 16), in relation to Eq. 6.

E. Object geometry to synergies transformation

The geometry of different objects acts as an environmental descriptor i.e, via-points and end-points for the reference synergistic trajectory $(e_n | t)$ as described in the previous section. Since, the dimensions of the object are in real coordinates and thus need to be transformed into respective synergistic

F. Synergy to Joint Space Mapping

Once the kernelized synergies for a particular task are determined, the next step is to command the robot hand to execute it. To comply with the hand joint control, the mapping
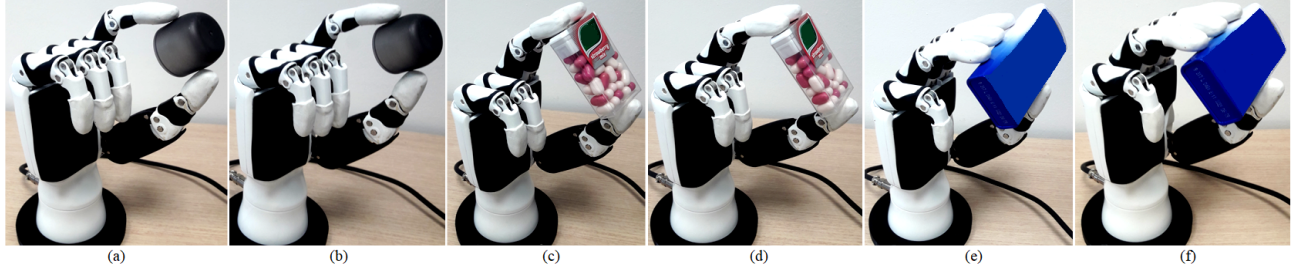
Fig. 7: Practical interpretations of the grasp quality index in the kernelized synergies framework on an anthropomorphic robot hand, (a), (c), and (e) represent the robot hand grasping objects in bipodal, tripodal and quadrapodal postures without considering the cost function ($\Gamma(\Delta e)$) and in (b), (d), and (f) the given cost function ($\Gamma(\Delta e)$) is used to improve the configuration that fingers adopt on the object surface.

is performed from the synergistic subspace to the joint space using Eq. 12

$$q = \hat{E}e + \vartheta^0 \quad (12)$$

Where, ϑ^0 denotes the initial robot hand joint vector. It must be noted that the dimensions of $\hat{E}$ depend upon the number of postural synergies considered (i.e, two in our case based on 85% variance criteria) to approximate the respective grasping and manipulation configurations.

IV. GRASP STABILITY ANALYSIS

The desired contact forces are not only required to hold the object in a stable position but also to avoid damage to the object or the robot itself. The joint torque of a DC motor is related to its current by $\tau = K_m I^2$, where K_m is the motor design constant. According to differential kinematics, the relationship between contact forces and joint torques is defined by $f_c = J_h \tau$. Therefore, there exists a kineto-static duality between the synergistic forces and velocities and hence the force synergies $\eta \in \mathbb{R}^{n_s}$ are given by Eq. 13.

$$\eta = \hat{E}^T J_h{}^T f_c \quad (13)$$

With the model in Eq. 13, the co-efficients of the kernelized synergies are modulated until the steady state contact forces are obtained. This must occur within the defined threshold on the motor current to ensure the grasp stability. Moreover, the force closure property is considered to evaluate the grasp quality of the proposed framework [33]. The problem is formulated as minimizing the cost function Γ to ensure the grasp stability. The general solution to the problem of contact forces balancing the grasped object is described by Eq. 14

$$f_c = G^\dagger \omega + \xi \Delta q_{ref} \quad (14)$$

Where, $G^\dagger$ is the pseudo-inverse of the grasp matrix and Δq_{ref} is the change in joint reference position. The matrix ξ maps the joint positions to the internal forces generated during the hand-object interaction. Now, the change in the joint positions can be defined in the synergistic subspace by $\Delta q_{ref} = S \Delta e$ and $\Delta q = \Delta q_{ref} - C_h \Delta \tau$, which is the model of soft synergies. The grasping problem can now be formulated in terms of the synergistic control framework by Eq. 15

$$f_c = G^\dagger \omega + \xi \Delta e \quad (15)$$

With reference to Eq. 15 and using the Coulomb's friction cone criteria, the synergy-based grasp quality index using force closure property is defined as minimizing Γ with respect to Δe. Let $\Omega^p_{i,j} \in \mathbb{R}^k$ represents the set of grasp variables (i.e, the synergistic coefficients e) that fulfill the friction cone constraints σ with a small positive margin p, where k is the dimension of ξ. Intuitively, σ defines the ratio between the normal and tangential forces applied by the robot hand on a given object, that need be within the pre-defined threshold to avoid slippage. Therefore, for the $i-th$ contact and $j-th$ constraint, Γ is the summation of terms: $\Gamma(\omega, e) = \sum_i \sum_j \Gamma_{i,j}(\omega, e)$, defined by Eq. 16 [34]

$$\Gamma_{i,j} = \begin{cases} (2\sigma^2_{i,j}(\omega, e))^{-1} & e \in \Omega^p_{i,j} \\ a\sigma^2_{i,j}(\omega, e) + b\sigma_{i,j}(\omega, e) + c & e \notin \Omega^p_{i,j} \end{cases} \quad (16)$$

Where, a, b, and c are the constants conditioned by the properties of Γ. The inverse of Γ is the grasp margin limit which must be respected to prevent violation of the friction cone constraints. It is essential in planning the dexterous manipulation. Note that, the contact points between the robot hand and objects are arbitrarily being defined by a human subject based on their experience, which ensures that they resemble the real ones and are iteratively updated to minimize Γ. However, in the absence of perceptual feedback, the contact information for all the objects (training, testing and experimenting) is manually being defined but it has nothing to do with the performance and robustness of the kernelized synergies framework. The framework can incorporate different sensory modalities that update the information about the environment (objects and surroundings) in Eq. 11, depending upon the nature of tasks, system conditions and user preferences [35][36].

To incorporate the force closure property into the kernelized synergies, the second correction term from Eq. 16 is included in the desired reference synergistic trajectory, such that the movements of the fingers are against the gradient of Γ. The main goal is to reproduce the synergistic movements that minimize Γ and this is formulated by Eq. 17, with $\kappa_q < 0$ being a constant gain, chosen experimentally according to the system dynamics.

$$\Delta e = \kappa_q \frac{\partial \Gamma}{\partial e} \Delta t \quad (17)$$

To understand the practical implementation and evaluation of $\Gamma(\Delta e)$, the anthropomorphic robot hand in Fig. 5 (a) is used to perform grasping of distinct objects in different postures,
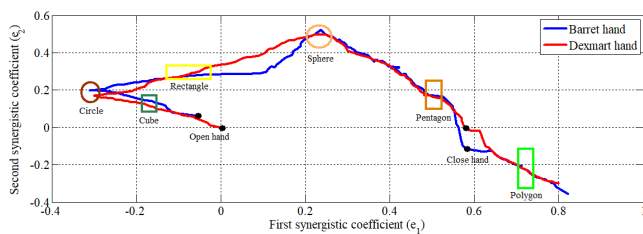
Fig. 8: Training trajectories of two principal synergistic coefficients for the Barrett and Dexmart hands using given geometrical objects.

as shown in Fig. 7. It is evident from Fig. 7 that the robot hand fingers are more evenly distributed around the surface of objects by using cost function $\Gamma(\Delta e)$ in Fig. 7 (b, d, f) than without it in Fig. 7 (a, c. e). This is due to the fact that the distance between the fingers and the centroid of the object is reduced and thus the area of the polygon formed by these finger contact points is improved. In the following section, the application of $\Gamma(\Delta e)$ is numerically evaluated on two different robot hand models in the Syngrasp toolbox, which gives an enriched understanding of how it improves the grasp stability. The improved grasp stability is shown by the reduced values of Γ, which is due to the optimized kerenlized synergistic control, according to Eq. 17.

V. SIMULATION ANALYSIS

The proposed framework of kernelized synergies is numerically evaluated on two different robot hand models in the SynGrasp MATLAB toolbox [37]. The first model is an anthropomorphic under-actuated Dexmart hand having 20 DoF with size and kinematics structure very similar to a human hand [38]. The other model is a Barrett Hand, which is a three fingered fully actuated robot hand with 8 joints and 4 DOFs [39]. Both the robot hand models are trained using the same geometrical objects, as shown in Fig. 4 and the corresponding trajectories of the synergistic coefficients are reported in Fig. 8. The simulations are performed with MATALAB2019b on a 2.6-GHZ Intel Core i5, 8-GB RAM computer.

To examine the application of kernelized synergies on the given robot hand models, the precision grasping and manipulation (rotation) of three distinct objects, of different shapes and sizes i.e, cube, sphere and cylinder, are considered in Fig. 9. Due to the compliance, introduced by the kernelized synergies, the contact forces between the object and hand are compensated for using the hard finger contact model, according to Eq. 15. It can be seen in Fig. 9 that both the hands are able to adapt to the varying dimensions of objects and also maintain the grasp stability according to force closure optimization criteria in Eq. 17. The logarithmic values of centroid (polygon formed by contact points between the hand and object) independently and then together with $\Gamma(\Delta e)$, computed for all the different grasps, on both the robot hands are reported in Table. II. It is evident from Table. II that the use of the force closure quality index ($\Gamma(\Delta e)$) significantly improves the grasp stability thereby reducing the unnecessary margin at the contact points (centroid). Moreover, the reduced values of (centroid+$\Gamma(\Delta e)$) when using the Dexmart hand confirm its better performance for stably grasping and manipulating objects due to its greater dexterity as compared to Barrett hand.

TABLE II: Quantitative computation of force closure quality index for both the robot hand models.

Hand	Object	Grasp	Centroid	Centroid+$\Gamma(\Delta e)$
Barret	Cube	Tripodal	6.2×10^8	2.3×10^7
	Sphere	Bipodal	5.1×10^7	3.7×10^6
	Cylinder	Tripodal	2.6×10^9	4.1×10^7
Dexmart	Cube	Tripodal	2.8×10^8	1.7×10^6
	Sphere	Bipodal	8.7×10^6	6.5×10^5
	Cylinder	Quadrapodal	1.8×10^9	2.2×10^7

The kernelized synergistic profile of the Dexmart hand, when grasping and manipulating the objects is shown in Fig. 10. Figs. 10 (a and b) show the trajectories of two synergistic coefficients computed using Eq. 2, that evolve over the total duration of the demonstrations. In order to find the correlation among such synergistic trajectories, the GMM is applied according to Eq. 3. This is illustrated in Fig. 10 (c), where the red ellipses are the corresponding Gaussian components approximating the given synergistic trajectories. For such probabilistic trajectories, to achieve the desired poses under different conditions, the reference trajectory in Fig. 10 (d) is determined using Eq. 4. For any new object, the proposed framework updates the via points and end points of the reference trajectory according to Eq. 7 such that the new object can be grasped and manipulated, as shown in Fig. 10 (e). Figs. 10 (f and g) represent the updated trajectories of two synergistic components for the selected three objects and their corresponding synergistic velocity profiles with desired via-points being marked in Figs. 10 (h and i). It is evident from the synergistic velocities that the hand experiences an overshoot for a short duration when it breaks contact with the objects. Such a behaviour is observed primarily due to two reasons; (i) the release of energy stored as tension in the tendons of the hand, and (ii) the change in inertia of the robot hand fingers, which arises during the transition from a contact to a non-contact state. However, it also reflects that the PD gains of the low level robot hand controller are properly tuned. This means that there is only a small overshoot with a short settling time.

VI. RESULTS AND DISCUSSION

To experimentally evaluate the performance of the proposed framework, four distinct complex interaction tasks are considered. All the tasks are still based on the basic grasping and manipulation primitives taught to the robot hand. Note that the appropriate values of the synergistic co-efficient e_g and e_m in all the following experiments are determined according to Eq. 11. However, Eq. 11 partially depends upon the dimensions of the working object and thus for each task, the values of e_g and e_m happen to be different but are still the members of the computed reduced synergistic subspace $\hat{E}$.

For task1, the robot hand utilizes its rotation manipulation primitives to pour the coffee from the paper cup into the glass and to close a jar, as shown in Fig. 11 and Fig. 12 respectively. For the coffee pouring task, the robot hand holding the paper coffee cup with $e_{g1} = 0.46, e_{g2} = 0.17$, is required to pour the coffee into empty glass on the table in Fig. 11 (a). The paper coffee cup is oriented with $e_{m1} = 0.47$ to 0.54,
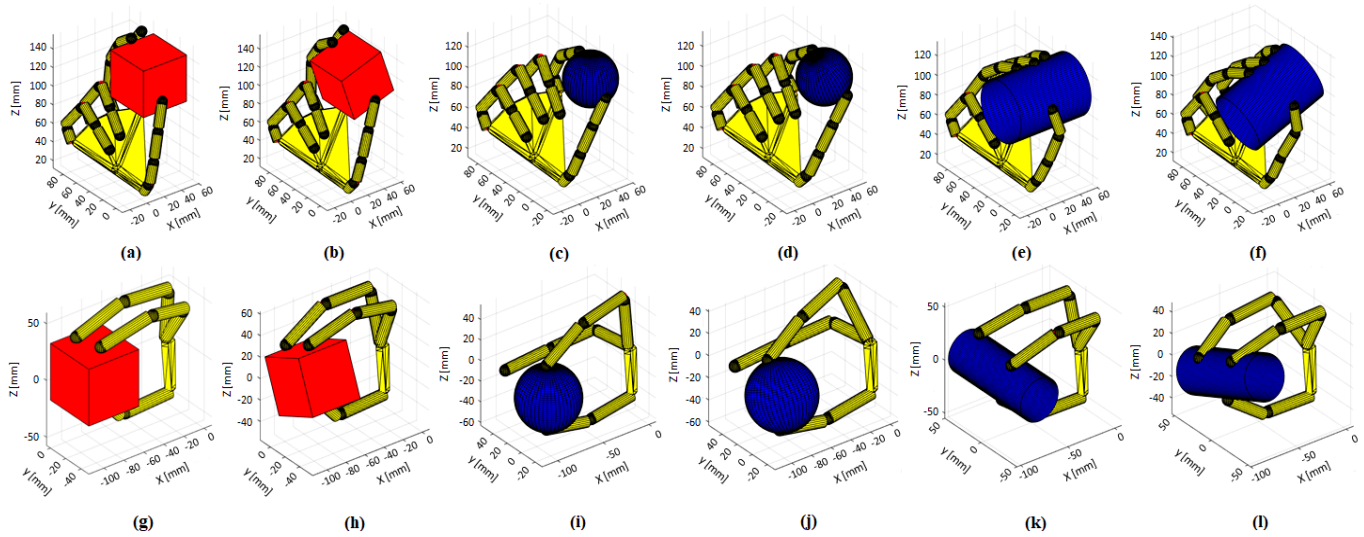
Fig. 9: Simulation analysis of kernelized synergies for two different robot hands. In the first row (a-f), the Dexmart hand is grasping and manipulating (rotating) three distinct objects of different shapes and sizes and in the second row (g-l), the Barrett hand is performing similar actions on the given objects but due to its limited dexterity it only exhibits two different postures i.e, bipodal and tripodal except quadrapodal
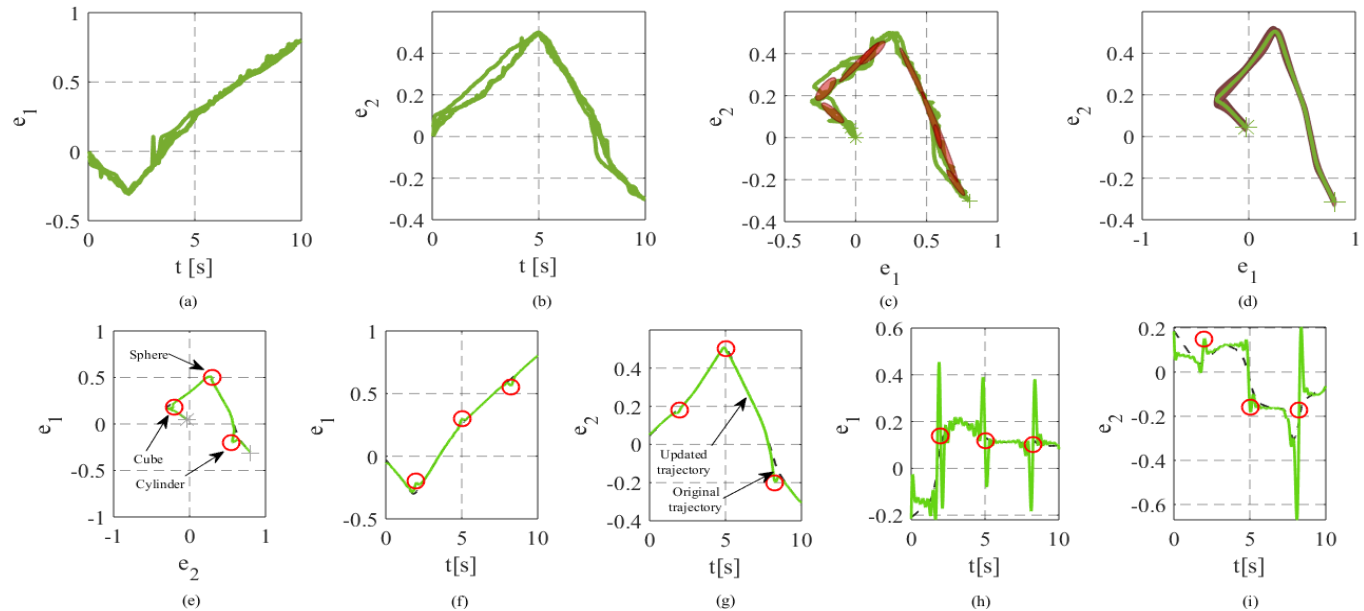

Fig. 10: Kernelized synergistic profile of the Dexmart hand when grasping and manipulating three objects, (a and b) represent the trajectories of the first two synergistic coefficients on the training data set, (c) is the relative trajectory approximated by Gaussian components shown in red ellipses , (d) is the final reference trajectory generated by the GMR with its mean value shown by the green curve and the range of its variance indicated by the shaded red area, (e) is the updated reference trajectory for grasping and manipulation (rotation) of the three distinct objects, (f-g) are the parametric synergistic trajectories reproduced over the set of three via-points (for three objects), (h-i) show the velocities of corresponding synergistic coefficients during interactions (contact and non-contact states) with the objects.

$e_{m2} = 0.18$ to 0.27 and the coffee starts to flow into a glass gradually depending upon the degree of orientation of fingers, as demonstrated in Figs. 11 (b) and (c). Finally, the cup is rotated backwards with $e_{m1} = 0.54$ to 0.47, $e_{m2} = 0.27$ to 0.18 so that only the required amount of coffee is poured into a glass, as shown in Fig. 11 (d). When closing the jar in Fig. 12 (a), the robot hand first grasps the lid with $e_{g1} = -0.27, e_{g2} = 0.16$ and then places it on top of the jar at a desired position, as shown in Figs. 12 (b) and (c) respectively. Finally, the robot hand turns the lid in a clockwise direction at $e_{m1} = -0.31$ to -0.39, $e_{m2} = 0.17$ to 0.21, to

screw it onto the jar, as illustrated in Fig. 12 (d). It must be noted that both the tasks are performed primarily with the fingers without any compensation at the wrist level.

During task2, the robot hand uses its translation manipulation primitives to open the toolbox latches with the required pulling action, as shown in Fig. 13. Fig. 13 (a) illustrates the toolbox with latches that are initially closed as marked in yellow and the robot hand first assumes the desired pose at $e_{g1} = -0.12, e_{g2} = 0.25$ and then opens the first and second latches with its index and middle fingers at $e_{m1} = 0.16$ to 0.23, $e_{m2} = -0.17$ to -0.05 by utilizing its translation prim-
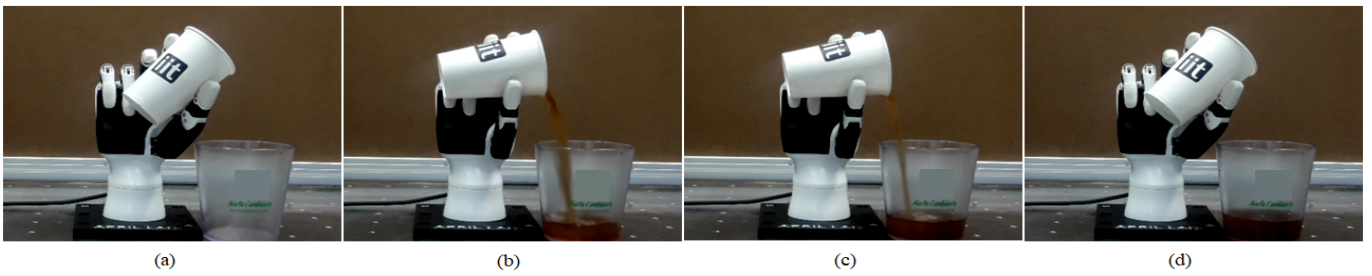
Fig. 11: A robot hand pouring coffee from a paper cup into a glass, (a) illustrates the initial configuration of the hand when grasping the coffee cup and the empty glass on the table, (b and c) show the flow of coffee into the glass at a rate determined by the relative movements of the fingers, (d) demonstrates the reoriented pose of coffee cup to stop the flow of coffee into the glass

Fig. 12: A robot hand closing a jar, (a) illustrates the jar and its lid, (b) demonstrate the robot hand grasping the lid in a tripod (3 fingered) precision grasp, (c) shows the scenario where the lid is placed on the jar while maintaining a stable grasp, (d) displays the final pose of jar with the lid being screwed onto it.
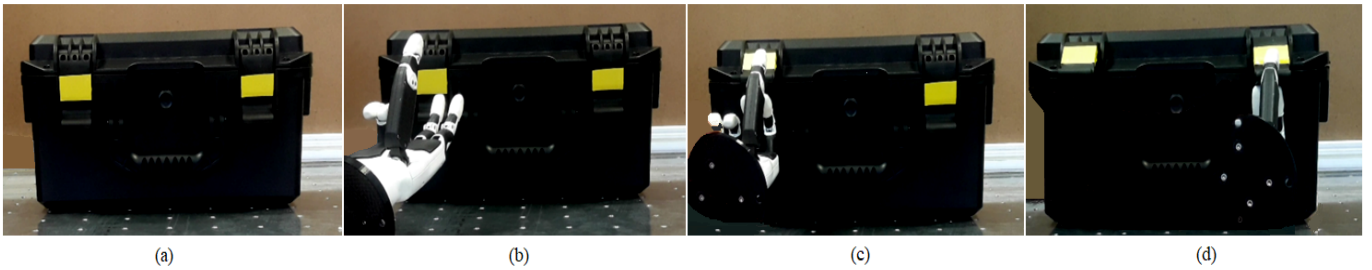

Fig. 13: A robot hand opening a toolbox using its learned translation manipulation primitive from the kernelized synergy subspace, (a) is the toolbox with both of its latches closed initially, (b) represents the scenario in which the robot hand assumes a tripod (3 fingered) pose with its little and ring fingers being closed, (c) illustrates the robot hand opening the first latch of toolbox with its index and middle fingers, (d) shows the similar robot hand action to open the second latch.

itives to generate the corresponding outward force, as shown in Figs. 13 (b), (c) and (d) respectively. Due to the compliance introduced by the kernelized synergies, the interaction between the fingertips and the latches is modulated from 0.85 N/sec to 1.23 N/sec during the pulling action, according to Eq. 15.

Task3 is about assigning priorities to the synergistic components according to Eq. 8 to grasp two objects sequentially and then manipulate one of them while maintaining a stable grasp, as shown in Fig. 14. In this case, the kernelized synergies exploit their priority characteristics to close two parts of the hand separately to grasp and manipulate distinct objects consecutively. Fig. 14 (a) illustrates the open hand configuration at $e_{g1} = e_{g2} = e_{m1} = e_{m2} = 0$, with both e_{g1} and e_{g2} having priority $\Upsilon = 0.5$. This allows the hand to close its two parts separately, as shown in Fig. 14 (b), where the robot hand grasps the first object with the little and ring fingers at $e_{g1} = -0.04, e_{g2} = 0.05$ and then it grips the second object in the tripod posture with $e_{g1} = -0.11, e_{g2} = 0.22$, in Fig. 14 (c). Finally, the second object is rotated clockwise at $e_{m1} = -0.02$ to 0.11, $e_{m2} = 0.25$ to 0.36 such that it

is manipulated without disturbing the pose of the first object in Fig. 14 (d). These features of kernelized synergies help in performing different multi-digit tasks such as writing with a pencil while holding a rubber, tightening a bolt while griping an extra nut, holding and pressing a spray and many others.

In task4, the robot is playing the board game "carrom", as shown in Fig. 15. This task requires precise grasping of the striker to move it to the desired position of attack and then perform the appropriate pushing motion, needed to guide the striker towards the goal pieces on the board. In Fig. 15 (a), the robot hand grasps the striker at $e_{g1} = -0.24, e_{g2} = 0.18$. It is then moved to a desired position on the board using the robot arm motion, as illustrated in Fig. 15 (b). The robot hand releases the striker at this desired location with $e_{g1} = -0.19, e_{g2} = 0.14$. The robot arm assumes the pose to bring the fingertips of the robot hand near the striker edge, as shown in Fig. 15 (c). The robot hand first stretches the fingers at $e_{m1} = 0.51$ to 0.59, $e_{m2} = 0.05$ to -0.08 in Fig. 15 (d) and then releases its index and middle fingers, and thumb at $e_{m1} = 0.1$ to -0.07, $e_{m2} = -0.04$ to 0.08 such that the striker
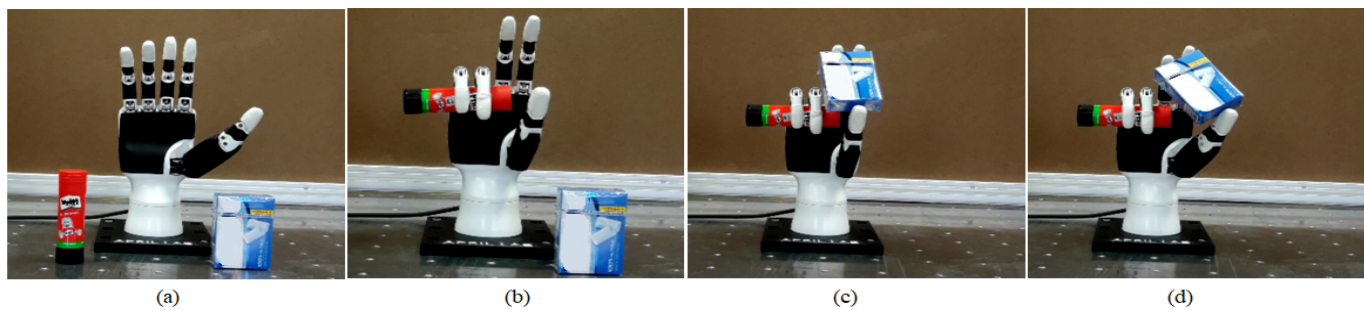
Fig. 14: A robot hand controls its two parts independently by assigning priories to the synergistic components to grasp two different objects sequentially and manipulating one of them, (a) is the open hand configuration of the robot hand, (b) shows the grasping of the first object with the little and ring fingers, (c) is the sequential grasping of the second object with the thumb, index and middle fingers in a tripod configuration, (d) illustrates the clockwise orientation of the second object using its manipulation rotation primitive.
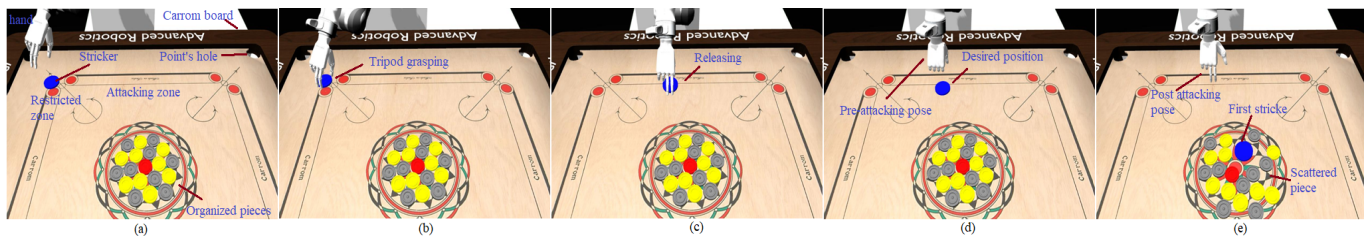

Fig. 15: Robot playing the carrom board game with the proposed framework, (a) is the initial configuration of the hand and striker in a restricted zone, (b) shows the hand grasping the striker with its thumb, index, and middle fingers in one of its taught precision postures, (c) shows the pose of hand when releasing the striker in the attacking zone, (d) represents the pose of hand which is stretched to develop the required pushing force, (e) illustrates the pushing action of the hand on the striker which leads it to the center to spread the pieces.

gets pushed towards the pieces in the center, as shown in Fig. 15 (e). The surface of the board is smooth and the friction between the striker and board is ignored, which is normal in this game. The weight of the striker is 15 grams, so a force of 1.25 N, calculated using robot hand's motor currents, is applied to push the striker towards the center. The pushing motion in this task corresponds to the general postures taught to the robot in the free hand configuration during the training phase in Fig. 4.

VII. CONCLUSIONS

This research has proposed, developed and tested a new framework, called kernelized synergies to address the limitations in using postural synergies for complex interaction tasks. In particular, it deals with the issues of convergence and computation constraints and their subsequent deficiency when performing continuous trajectorial tasks i.e, manipulations. This framework instead of determining new synergies, reuses the same learned synergy subspace for both precision grasping and dexterous manipulation of distinct daily life objects.

In the development of the kernelized synergies framework, the postural synergies, computed by tele-operating the robot hand during elementary grasping and manipulation primitives, evolved over the duration of the demonstrations to obtain the corresponding synergistic trajectories. These synergistic trajectories were approximated using a GMM-GMR model in terms of Gaussian components. This not only takes into account the inconsistencies in the demonstrations but also learns a generalized probabilistic trajectory that can be used to reproduce the taught postures during model inference. However, to grasp and manipulate a new object, the KMP was exploited to deal with

environmental descriptors i.e, via-points and end-points, and hence was able to adapt to the new shape and size respectively. The parametric synergistic trajectory, kernelized by the KMP, preserved the grasping and manipulation characteristics so that the same computed synergistic subspace can be reused for new objects. The proposed framework was initially tested in simulated environments using the Syngrasp toolbox on two different robot hand models. The stability of postures was evaluated and reported using a force closure quality index. The lower values of this metric for an anthropomorphic robot hand indicated its higher dexterity on stably grasping objects. For real-time experimental evaluation, four complex tasks similar to the daily life activities i.e, pouring coffee and closing a jar, opening toolbox latches, sequentially grasping and manipulating two objects, and playing the carrom board game, were performed and discussed. The results confirm that the proposed framework bridges the gap between the grasping and manipulation sub-spaces and is a hand agnostic approach provided the demonstration are carried out on the robot hand of interest.

Current limitations of proposed frame, include manual inception of grasping points, the approximation of the joint torques from the fingertips' positions, and testing for a small number of rigid daily life objects. Future work will seek to address these shortcomings through the use of combined and integrated visual and tactile information to incorporate runtime object detection, pose estimation and adaptation to a dynamic environment. This will also consider fine manipulation of a greater range of objects including soft objects. In addition, the capacity of the current framework to prioritize different tasks at different levels will be exploited in motion planning

of non-holonomic co-manipulation tasks. Finally, other kernel functions will be tested to examine their effects on performance and robustness in dealing with complex prehensile and non-prehensile manipulation tasks.

REFERENCES

[1] A. Bicchi, M. Gabiccini, and M. Santello, "Modelling natural and artificial hands with synergies," *Philosophical Transactions of the Royal Society B: Biological Sciences*, vol. 366, no. 1581, pp. 3153–3161, 2011.

[2] J. T. Belter, J. L. Segil, and B. SM, "Mechanical design and performance specifications of anthropomorphic prosthetic hands: a review," *Journal of rehabilitation research and development*, vol. 50, no. 5, p. 599, 2013.

[3] A. Bicchi, "Hands for dexterous manipulation and robust grasping: A difficult road toward simplicity," *IEEE Transactions on robotics and automation*, vol. 16, no. 6, pp. 652–662, 2000.

[4] J. Bohg, A. Morales, T. Asfour, and D. Kragic, "Data-driven grasp synthesis—a survey," *IEEE Transactions on Robotics*, vol. 30, no. 2, pp. 289–309, 2013.

[5] F. Ficuciello, D. Zaccara, and B. Siciliano, "Synergy-based policy improvement with path integrals for anthropomorphic hands," in *2016 IEEE/RSJ International Conference on Intelligent Robots and Systems (IROS)*. IEEE, 2016, pp. 1940–1945.

[6] F. Ficuciello, A. Migliozzi, G. Laudante, P. Falco, and B. Siciliano, "Vision-based grasp learning of an anthropomorphic hand-arm system in a synergy-based control framework," *Science robotics*, vol. 4, no. 26, 2019.

[7] M. Santello, M. Flanders, and J. F. Soechting, "Postural hand synergies for tool use," *Journal of neuroscience*, vol. 18, no. 23, pp. 10 105–10 115, 1998.

[8] F. Ficuciello, A. Federico, V. Lippiello, and B. Siciliano, "Synergies evaluation of the schunk s5fh for grasping control," in *Advances in Robot Kinematics 2016*. Springer, 2018, pp. 225–233.

[9] C. O. S. Sorzano, J. Vargas, and A. P. Montano, "A survey of dimensionality reduction techniques," *arXiv preprint arXiv:1403.2877*, 2014.

[10] S. Velliangiri, S. Alagumuthukrishnan *et al.*, "A review of dimensionality reduction techniques for efficient computation," *Procedia Computer Science*, vol. 165, pp. 104–111, 2019.

[11] G. Salvietti, "Replicating human hand synergies onto robotic hands: A review on software and hardware strategies," *Frontiers in neurorobotics*, vol. 12, p. 27, 2018.

[12] F. Ficuciello, G. Palli, C. Melchiorri, and B. Siciliano, "Postural synergies of the ub hand iv for human-like grasping," *Robotics and Autonomous Systems*, vol. 62, no. 4, pp. 515–527, 2014.

[13] G. Cotugno, V. Mohan, K. Althoefer, and T. Nanayakkara, "Simplifying grasping complexity through generalization of kinaesthetically learned synergies," in *2014 IEEE International Conference on Robotics and Automation (ICRA)*. IEEE, 2014, pp. 5345–5351.

[14] I. Cerulo, F. Ficuciello, V. Lippiello, and B. Siciliano, "Teleoperation of the schunk s5fh under-actuated anthropomorphic hand using human hand motion tracking," *Robotics and Autonomous Systems*, vol. 89, pp. 75–84, 2017.

[15] B. D. Argall, S. Chernova, M. Veloso, and B. Browning, "A survey of robot learning from demonstration," *Robotics and autonomous systems*, vol. 57, no. 5, pp. 469–483, 2009.

[16] M. G. Catalano, G. Grioli, E. Farnioli, A. Serio, C. Piazza, and A. Bicchi, "Adaptive synergies for the design and control of the pisa/iit softhand," *The International Journal of Robotics Research*, vol. 33, no. 5, pp. 768–782, 2014.

[17] C. Piazza, C. Della Santina, M. Catalano, G. Grioli, M. Garabini, and A. Bicchi, "Softhand pro-d: Matching dynamic content of natural user commands with hand embodiment for enhanced prosthesis control," in *2016 IEEE International Conference on Robotics and Automation (ICRA)*. IEEE, 2016, pp. 3516–3523.

[18] G. Gioioso, G. Salvietti, M. Malvezzi, and D. Prattichizzo, "Mapping synergies from human to robotic hands with dissimilar kinematics: an approach in the object domain," *IEEE Transactions on Robotics*, vol. 29, no. 4, pp. 825–837, 2013.

[19] N. Jarrassé, A. T. Ribeiro, A. Sahbani, W. Bachta, and A. Roby-Brami, "Analysis of hand synergies in healthy subjects during bimanual manipulation of various objects," *Journal of neuroengineering and rehabilitation*, vol. 11, no. 1, pp. 1–11, 2014.

[20] M. Ewerton, O. Arenz, G. Maeda, D. Koert, Z. Kolev, M. Takahashi, and J. Peters, "Learning trajectory distributions for assisted teleoperation and path planning," *Frontiers in Robotics and AI*, vol. 6, p. 89, 2019.

[21] C. Della Santina, M. Bianchi, G. Averta, S. Ciotti, V. Arapi, S. Fani, E. Battaglia, M. G. Catalano, M. Santello, and A. Bicchi, "Postural hand synergies during environmental constraint exploitation," *Frontiers in neurorobotics*, vol. 11, p. 41, 2017.

[22] F. Ficuciello, G. Palli, C. Melchiorri, and B. Siciliano, "Postural synergies and neural network for autonomous grasping: a tool for dextrous prosthetic and robotic hands," in *Converging Clinical and Engineering Research on Neurorehabilitation*. Springer, 2013, pp. 467–480.

[23] G. Palli, F. Ficuciello, U. Scarcia, C. Melchiorri, and B. Siciliano, "Experimental evaluation of synergy-based in-hand manipulation," *IFAC Proceedings Volumes*, vol. 47, no. 3, pp. 299–304, 2014.

[24] C. Della Santina, C. Piazza, G. Grioli, M. G. Catalano, and A. Bicchi, "Toward dexterous manipulation with augmented adaptive synergies: The pisa/iit softhand 2," *IEEE Transactions on Robotics*, vol. 34, no. 5, pp. 1141–1156, 2018.

[25] G. Z. Gandler, C. H. Ek, M. Björkman, R. Stolkin, and Y. Bekiroglu, "Object shape estimation and modeling, based on sparse gaussian process implicit surfaces, combining visual data and tactile exploration," *Robotics and Autonomous Systems*, vol. 126, p. 103433, 2020.

[26] F. Ficuciello, G. Palli, C. Melchiorri, and B. Siciliano, "A model-based strategy for mapping human grasps to robotic hands using synergies," in *2013 IEEE/ASME International Conference on Advanced Intelligent Mechatronics*. IEEE, 2013, pp. 1737–1742.

[27] (2018) Inspire robots technology co.,ltd. [Online]. Available: http://www.inspirerobots.com/product/278016338

[28] S. Calinon, F. Guenter, and A. Billard, "On learning, representing, and generalizing a task in a humanoid robot," *IEEE Transactions on Systems, Man, and Cybernetics, Part B (Cybernetics)*, vol. 37, no. 2, pp. 286–298, 2007.

[29] A. Billard, S. Calinon, R. Dillmann, and S. Schaal, "Survey: Robot programming by demonstration," Springer, Tech. Rep., 2008.

[30] Y. Huang, L. Rozo, J. Silvério, and D. G. Caldwell, "Kernelized movement primitives," *The International Journal of Robotics Research*, vol. 38, no. 7, pp. 833–852, 2019.

[31] A. M. Okamura, N. Smaby, and M. R. Cutkosky, "An overview of dexterous manipulation," in *Proceedings 2000 ICRA. Millennium Conference. IEEE International Conference on Robotics and Automation. Symposia Proceedings (Cat. No. 00CH37065)*, vol. 1. IEEE, 2000, pp. 255–262.

[32] G. Gioioso, G. Salvietti, M. Malvezzi, and D. Prattichizzo, "An object-based approach to map human hand synergies onto robotic hands with dissimilar kinematics," in *Robotics: Science and Systems VIII*. The MIT Press Sydney, NSW, 2012, pp. 97–104.

[33] A. Bicchi, "On the closure properties of robotic grasping," *The International Journal of Robotics Research*, vol. 14, no. 4, pp. 319–334, 1995.

[34] F. Ficuciello, "Synergy-based control of underactuated anthropomorphic hands," *IEEE Transactions on Industrial Informatics*, vol. 15, no. 2, pp. 1144–1152, 2018.

[35] A. Saxena, L. Wong, M. Quigley, and A. Y. Ng, "A vision-based system for grasping novel objects in cluttered environments," in *Robotics research*. Springer, 2010, pp. 337–348.

[36] G. Du, K. Wang, S. Lian, and K. Zhao, "Vision-based robotic grasping from object localization, object pose estimation to grasp estimation for parallel grippers: a review," *Artificial Intelligence Review*, vol. 54, no. 3, pp. 1677–1734, 2021.

[37] M. Malvezzi, G. Gioioso, G. Salvietti, and D. Prattichizzo, "Syngrasp: A matlab toolbox for underactuated and compliant hands," *IEEE Robotics & Automation Magazine*, vol. 22, no. 4, pp. 52–68, 2015.

[38] G. Palli, C. Melchiorri, G. Vassura, U. Scarcia, L. Moriello, G. Berselli, A. Cavallo, G. De Maria, C. Natale, S. Pirozzi *et al.*, "The dexmart hand: Mechatronic design and experimental evaluation of synergy-based control for human-like grasping," *The International Journal of Robotics Research*, vol. 33, no. 5, pp. 799–824, 2014.

[39] (2008) The barrett hand, barrett technologies, inc., cambridge, ma, usa. [Online]. Available: https://advanced.barrett.com/barretthand

Sunny Katyara has received his bachelors from Mehran University of Engineering and Technology, Pakistan and masters from Wroclaw University of Science and Technology, Poland in 2015 and 2018 respectively. He is a PhD student jointly supervised by PRISMA Lab and ADVR IIT, Italy. Mr. Katyara has published more than 20 research articles in international journals and conferences. His research interests include; anthropomorphic fine manipulations, Bayesian inference controllers, human-robot interaction and sim2real skill transfer.

Fanny Ficuciello received the Laurea degree magna cum laude in Mechanical Engineering and the Ph.D. degree in Computer and Automation Engineering both at the University of Naples Federico II in 2007 and 2010 respectively. Currently, she is Assistant Professor of Robotics and Automation at the University of Naples Federico II. She is responsible of the scientific research in surgical robotics at the Robotics Lab of ICAROS Center (Interdepartmental Center for Advances in Robotic Surgery). She has published more than 90 journal and conference papers and book chapters. From 2017 she received the upgrade to IEEE Senior Member. From 2018 she is in the Technology Committee of the European Association of Endoscopic Surgery (EAES). Recently she held the position of Treasurer of ASME Italy Section. Currently she serves as Associate Editor for Journal of Intelligent Service Robotics (JIST) and for Transactions on Robotics (T-Ro).

Darwin G. Caldwell is Founding Director of the Italian Institute of Technology (IIT) in Genoa, Italy, where he is also the Director of the Dept. of Advanced Robotics. He is or has been an Honorary Professor at the University of Manchester, University of Sheffield, King's College London, and the University of Bangor in the UK, and Tianjin University and SAAT in China. His research interests include; innovative actuators, haptics, exoskeletons, medical, rehabilitation and assistive robotic technologies, human-robot interaction, dexterous manipulators, humanoid and quadrupedal robotics, telepresence and teleoperation, and food and agricultural robotics. Key robots developed by his group have included: iCub, a child-sized humanoid robot; COMAN, a compliant humanoid robot designed to safely interact with people; WALK-MAN, a 1.85m tall, 120kg humanoid that competed in the DARPA Robotics Challenge; the HyQ series (HyQ, HyQ2Max, HyQ-Real) of high performance hydraulic quadrupedal robots; and the Centauro, a "human-robot symbiotic system capable of robust locomotion and dexterous manipulation in the rough terrain and disasters" (e.g. earthquake, nuclear, chemical). He has published over 600 papers, 0ver 20 patents and has received over 50 awards/nominations at international conferences and events. His group has participated in over 30 European projects. He has served on the Editorial Boards of several journals as well as being Chair or Co-Chair for numerous international conferences and delivering over 50 keynote/plenary presentations. In 2015 Professor Caldwell was elected a Fellow of the Royal Academy of Engineering.

Bruno Siciliano is Professor of Control and Robotics, Director of the Interdepartmental Center for Advanced RObotics in Surgery (ICAROS) and Coordinator of the PRISMA Lab in the Department of Electrical Engineering and Information Technology at University of Naples Federico II. He is also Honorary Professor of Óbuda University, where he holds the Kálmán Chair. His research interests include robot manipulation and control, human–robot cooperation, and service robotics. He has co-authored/co-edited 18 books, more than 120 journal papers and more than 300 conference papers/book chapters; his book Robotics: Modelling, Planning and Control is one of the most widely adopted textbooks world-wide and has been translated into Chinese, Greek and Italian. He has delivered more than 30 keynotes, more than 150 invited lectures and seminars at institutions worldwide, and he has been the recipient of several awards. He is also a Fellow of ASME and IFAC. He is Co-Editor of the Springer Tracts in Advanced Robotics series, the Springer Proceedings in Advanced Robotics series, and has served on the Editorial Boards of several journals as well as Chair or Co-Chair for numerous international conferences. He co-edited the Springer Handbook of Robotics, which received the AAP PROSE Award for Excellence in Physical Sciences & Mathematics and was also the winner in the category Engineering & Technology. His group has been granted more than twenty European projects, including an Advanced Grant from the European Research Council. He has served the IEEE Robotics and Automation Society as President, as Vice-President for Technical Activities and Vice-President for Publications, as a member of the AdCom, and as a Distinguished Lecturer. He has been a Board Director of the European Robotics Association. Professor Siciliano is currently an IFAC Pavel J. Nowacki Distinguished Lecturer and a member of the International Foundation of Robotics Research Board.

Fei Chen (S09'-M'12-SM'20) received the B.S. degree in computer science from Xi'an Jiaotong University (XJTU), Xi'an, China, in 2006, the M.S. degree in computer science from Harbin Institute of Technology (HIT), Harbin, China, in 2008, and the Dr. Eng. degree from Fukuda Laboratory, Micro-nano Systems Engineering, Nagoya University, Nagoya, Japan, in 2012. In June 2013, he joined the Department of Advanced Robotics within Italian Institute of Technology (IIT), Italy. He was the head of the Active Perception and Robot Interactive Learning (APRIL) laboratory with IIT. Since 2020, he has been working as an assistant professor leading the Smart Manipulation Robots (SMART) Laboratory, with T-Stone Robotics Institute (CURI), The Chinese University of Hong Kong (CUHK), as well as the Hong Kong Center for Logistics Robotics (HKCLR). His research interests lie in robot perception, learning, planning and control for various types of mobile manipulation. He is the co-chair of IEEE Robotics and Automation Society Technical Committee on Neuro-Robotics Systems, as well as chairs for several international conferences and workshops.